Ecological Modelling 350 (2017) 1–10

Contents lists available at ScienceDirect

Ecological Modelling

journal homepage: www.elsevier.com/locate/ecolmodel

A new temporal–spatial dynamics method of simulating land-use change

Dongya Liu [a], Xinqi Zheng [a,*], Chunxiao Zhang [a], Hongbin Wang [b]

[a] School of Information Engineering, China University of Geosciences, Beijing, China
[b] Institute of Network Technology, Beijing University of Posts and Telecommunications, Beijing, China

ARTICLE INFO

Article history:
Received 26 November 2016
Received in revised form 22 January 2017
Accepted 6 February 2017

Keywords:
Land-use change simulation
Temporal–spatial dynamics method
Cellular automata model
System dynamics model

ABSTRACT

The integration of a system dynamics (SD) model, a cellular automata (CA) model, and a Geographic Information System (GIS) is an important topic in the temporal and spatial simulation of land-use changes. Based on many previous studies, the temporal–spatial dynamics method (TSDM) has been proposed as a research framework that removes the limitations of using loosely coupled SD–CA–GIS. In this study, TSDM was successfully implemented in the NetLogo platform. The results show that: (1) Integration SD–CA–GIS based on grids leads to the seamless implementation of real-time data exchange among SD, CA, and GIS; (2) The temporal–spatial dynamic mechanisms can be represented using common time steps in SD–CA–GIS, and TSDM can be used for spatial visualization; and (3) The model accuracy can be improved by extending the CA transition rules with SD. The land-use patterns for 2000, 2010, and 2016 in Beijing, China, were simulated to test the TSDM implementation, and the simulation accuracies were 83.75%, 80.98%, and 77.40%, respectively. The results indicate that TSDM achieves a much better accuracy than conventional SD–CA–GIS coupled models, and is a more practical approach to simulate land-use change.

1. Introduction

Land-use change simulation is very useful for governmental plans and policies; it is also important for academic research. A number of models have been developed for the simulation of land-use change such as Markov chains (López et al., 2001), system models (Le et al., 2010), the SLEUTH (Hui-Hui et al., 2012), and the CLUES-S (Hu et al., 2013). A novel method based on a system dynamics (SD) model, a cellular automata (CA) model, and a Geographic Information System (GIS) is proposed in this study to deal with complex time-dependent phenomena.

GISs have strong spatial capturing, processing, and calculating capabilities and are applied to store, manage, and analyze spatial data (Zhang and Huang, 2014). The GIS is widely used for a variety of natural and social phenomena such as urban construction, land use, environment management, and macro-policy design (Clarke and Gaydos, 1998; Weng, 2002). Although GIS is powerful and has wide-ranging applications, it is not well adapted to representing time and cannot effectively capture model dynamics (An et al., 2005). This makes it difficult for GIS to simulate nonlinear and complex phenomena such as land-use change (Li et al., 2011). Therefore, it is required to identify complex, time-dependent phenomena by integrating GIS with other models.

The SD models offer a possibility for GIS extension in time; they are macro-dynamics models based on a "top-down" concept. Complex relationships among elements under different "what-if" scenarios can be simulated using SD and the flow and feedback relationships between various features can be expressed. The SD can be used to predict changes and build a dynamic simulation model based on observations. Recently, scholars have increasingly begun using SD to simulate complex land problems (Liu et al., 2013). However, SD models are macro-quantitative and neglect individual behavior. There is no spatial expression in SD. Therefore, it cannot readily handle spatial data; it also has difficulties in expressing and analyzing the interactions among spatial data (Guo et al., 2001).

As a "bottom-up" dynamic spatial system representation (White et al., 1997), cellular automata (CA) modeling is widely applied to simulate complicated dynamic systems (Arsanjani et al., 2013; Yang et al., 2012). The CA model contains four basic elements: cell, state, neighborhood, and transition rule. The cell is the smallest and most basic unit in CA. The state comprises a series of data values; each cell can only be in one specific state at a time point. Thus, the state is used to represent the current value of the cell (e.g. dead or alive). The other cells within a certain distance around the cen-

* Corresponding author at: 29# Xueyuan Road, Haidian District, Beijing, China.
E-mail address: zhengxq@cugb.edu.cn (X. Zheng).

http://dx.doi.org/10.1016/j.ecolmodel.2017.02.005
0304-3800/

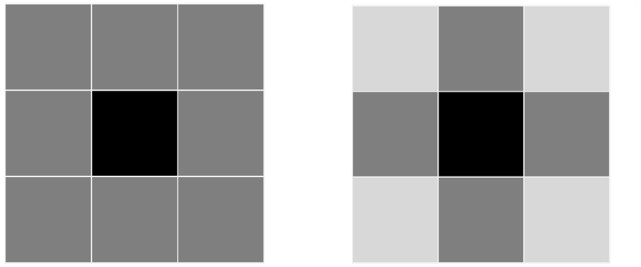

(a) Moore neighborhood (b) Von Neumann neighborhood

Fig. 1. The definition of CA neighborhood.

tral cell are referred to as the neighborhood. Nowadays, general neighborhoods used (Fig. 1) are the Moore neighborhood (containing eight contiguous cells) and the Von Neumann neighborhood (containing four basic contiguous cells; White and Engelen, 2000). The transition rule is a function that determines the state of the cell in the next moment; it is the core of CA. A variety of methods are used to define the transition rules, such as ant colony optimization (Yang et al., 2012), data mining (Li and Gar-On Yeh, 2004), logistic regression (Munshi et al., 2014), and artificial immune systems (Liu et al., 2010). The CA model is discrete in both time and space. All cells follow the same transition rules; the simple evolution of each cell contributes to define the complex change of the whole system. The CA has a strong spatial power. As CA is cell-based, it can easily be integrated with GIS. However, traditional CA has the following weaknesses: (1) In systems that attach importance to macro-driving factors, CA cannot readily address how macro-scale regulation, economic development, technical progress, and population migration influence micro-units (Ward et al., 2000). Also, CA cannot reflect the impact of micro-unit attribute changes on macro-factors; (2) The transition rules do not change during the simulation of the whole system. However, the transition rules need to change with time and also with different macro-states of the system in some scenarios (Theobald and Gross, 1994); and (3) All cells follow the same transition rules in traditional CA models; special cells are not distinguished. This is not appropriate for land-use studies; for example, some land, such as historical sites, is not free to change its use.

With respect to advantages and weaknesses of SD, CA, and GIS, some studies have integrated SD–CA–GIS, realizing simulations of both macro- and micro-characteristics of various complex systems (He et al., 2006; Han et al., 2009; Lauf et al., 2012). However, the models developed in these studies are mostly based on loose coupling between SD and CA. The two submodels work independently. There is a lack of effective feedback between SD and CA. The integration of the two submodels at a functional level is achieved by using the temporal character of SD and the spatial character of CA, but the effective iterative communication between SD and CA cannot be realized. The geographic system basic model (GSBM; Zheng, 2012) and the similar models integrated framework (Shen, 2006; Zhang et al., 2016) indicate, in theory, the potential of a closely coupled SD–CA–GIS.

For our purpose, in this paper, a temporal–spatial dynamics method (TSDM) is proposed based on previous research and its implementation is discussed. The TSDM is designed to provide integrated coupling of SD–CA–GIS. The TSDM was implemented based on the LOGO language using NetLogo as the development platform. The TSDM is used to simulate, forecast, and display geographical distributions; it can simulate the land-use change in multiple dimensions and at multiple scales. The TSDM establishes a coupled bidirectional communication mechanism between SD and CA. The TSDM was tested and validated using land-use data from 1990 to 2016 for Beijing. Section 2 mainly introduces the basic principle of TSDM and the concrete realization on the NetLogo platform. Section 3 describes the validation of the model based on the case of Beijing. Section 4 provides an in-depth discussion of the results. Conclusions are drawn in Section 5 and a future outlook is provided.

2. TSDM

2.1. General structure

Fig. 2 illustrates the temporal–spatial land-use changing process simulated by TSDM. The TSDM takes advantage of SD in the time dimension and, at the same time, integrates the characteristics of CA in the spatial dimension. The model also involves spatial visualization based on GIS. The TSDM can seamlessly integrate SD–CA–GIS by adopting a coordinating step between SD and CA and realizes temporal–spatial dynamic mechanisms and spatial visualization.

The TSDM builds on SD and simulates and analyzes based on system theory. The TSDM can simulate and predict time-dependent land macro factors under different "what-if" scenarios using macro-driving factors such as population policy, land policy, and economic development. The transition rules of CA are influenced by land macro elements obtained in SD and are combined with neighborhood and state considerations and mandatory constraints. The iterations of CA are also controlled by the SD land macro factors. All cells are iterated to simulate the next time state at a cell-scale; the land-use distribution is defined spatially. Based on this, relevant index parameters at the spatial-scale are calculated. The computed index parameters are fed back to SD and the next simulation step is initiated. This process is repeated until the simulation stops at the final year.

In TSDM, GIS, SD, and CA are integrated using the smallest grid element. The grid is the most basic element in TSDM and is also the key factor in model integration. The communication of geographic information during the integration of SD–CA–GIS is realized with grids. Micro-dimensional changes result in complex macro-dimension information and are reciprocally controlled by macro-dimension index factors. The general TSDM relationship can be expressed as:

$$F^{t+1} = \mathrm{f}(SD^{t+1}, CA^{t}), \tag{1}$$

where F^{t+1} is the land-use state at time $t+1$; SD^{t+1} represents the effect of land change by SD at time $t+1$, which is determined by SD^{t} and CA^{t}; CA^{t} denotes the effect of land change by CA at time t, which is determined by F^{t} and SD^{t+1}; and f is the transition function.

2.2. Rule structuring

The rules for data interaction between SD and CA have been extended in TSDM. The traditional integration of SD–CA–GIS can only control iterations of CA by using macro-driving factors that are simulated in SD. In the traditional integration, the time step is much longer and there is no feedback of the CA simulation results to SD, which could influence and adjust the operation of the proposed SD model.

The TSDM feeds the CA simulation data at the micro-scale back to SD and adjusts the simulation trends of the dynamic models in SD according to real-time data transfer between SD and CA. The TSDM combines SD with spatial data to improve the simulated and predicted precision of SD. At the same time, the CA real-time simulation ability is extended and the drawback of the CA transition rules being unchanged during the whole simulation is rectified because the CA transition rules are influenced by the SD driving factors. The iterations are controlled by SD macro-driving factors to ensure the authenticity and reliability of the CA simulation.

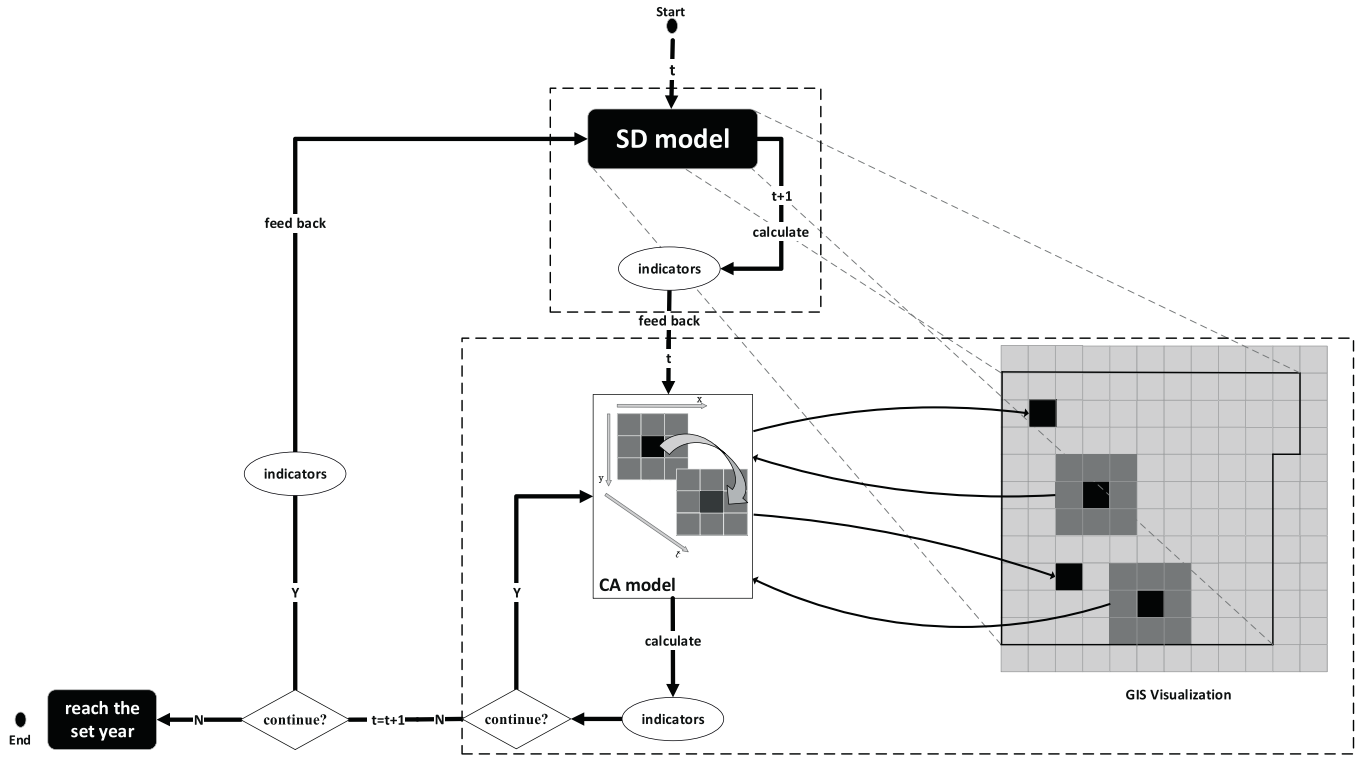

Fig. 2. The general TSDM structure.

The transition rules are the core and most important part of the CA model. The transition rules of the traditional CA can be written as:

$$S^{t+1} = \mathrm{f}(S^t, N^t), \tag{2}$$

where S^{t+1} is the cell state at time $t+1$; S^t is the cell state at time t; N^t refers to the neighborhood cell state at time t; and f is the transition function of the cell state from time t to time $t+1$.

This paper extends the effects of the SD driving factors to the CA transition rules. Therefore, the CA transition rules are calculated as:

$$S^{t+1} = \mathrm{f}(S^t, N^t, SD^{t+1}), \tag{3}$$

where SD^{t+1} is the effect of SD on the cell state at time $t+1$.

Also, this paper extends the CA transition rules by adding cell self-characteristics, mandatory constraints, and random interference factors to the CA to enlarge the basis of the traditional CA transition function and build an extended cellular automata model.

At time t, the probability $P_{k,t}$ of cell k transiting from state i to state j is defined by the function, which is determined by a cell neighborhood effect probability factor $N_{k,t}$, a transition probability factor $H_{k,t}$ determined by cell self-characteristics, a probability factor $C_{k,t}$ due to a mandatory constraints effect, a random interference probability factor $R_{k,t}$, and a probability factor $P_{SD,t+1}$ related to the SD influence. It can be expressed as follows:

$$P_{k,t} = \mathrm{f}(N_{k,t}, H_{k,t}, C_{k,t}, R_{k,t}, \mathrm{P_{SD,t+1}}), \tag{4}$$

The probability factor $H_{k,t}$, which is determined by cell self-characteristics, is calculated as follows:

$$H_{k,t} = \mathrm{f}(SE_{k,t}, SH_{k,t}), \tag{5}$$

where $SE_{k,t}$ reflects the influence of the surrounding environment (e.g., highway or railway) on the central cell and $SH_{k,t}$ is determined by the cell self-characteristics.

The mandatory constraints probability factor $C_{k,t}$ is:

$$C_{k,t} = \mathrm{f}(CE_{k,t}, CH_{k,t}, CP_{k,t}), \tag{6}$$

where $CE_{k,t}$ are the mandatory constraints produced by environmental factors; $CH_{k,t}$ are the mandatory constraints due to human factors (e.g., nature protection areas); and $CP_{k,t}$ are the mandatory constraints generated by national policies.

To simplify the operation, the above-mentioned equations can be summarized as (Li et al., 2014; Liao et al., 2016):

$$P_{k,t} = \sum_{h=1}^{w} N_{h,k,t} \times \sum_{m=1}^{n} SE_{m,k,t} \times SH_{k,t} \times \prod_{p=1}^{q} CE_{p,k,t} \times \prod_{r=1}^{s} CH_{r,k,t} \times \prod_{u=1}^{v} CP_{u,k,t} \times R_{k,t} \times P_{SD,t+1} \tag{7}$$

where $\sum_{h=1}^{w} N_{h,k,t}$ is the influence probability of the neighborhood cells; $N_{h,k,t}$ is the influence probability of neighborhood cell on the central cell; $\sum_{m=1}^{n} SE_{m,k,t}$ is the influence probability generated by the surrounding environment factors; $\prod_{p=1}^{q} CE_{p,k,t}$ are the mandatory constraints produced by the natural environment; $CE_{p,k,t}$ are binary data, where $CE_{p,k,t} = 0$ indicates that cell k is forcibly constrained by the natural environment, otherwise, $CE_{p,k,t} = 1$; $\prod_{r=1}^{t} CH_{r,k,t}$ are mandatory constraints produced by human factors; $CH_{r,k,t}$ are binary data, where $CH_{r,k,t} = 0$ means that cell k is strongly constrained by human factors, otherwise, $CH_{r,k,t} = 1$; $\prod_{u=1}^{v} CP_{u,k,t}$ are the mandatory constraints produced by national policies; and $CP_{u,k,t}$ are binary data, where $CP_{u,k,t} = 0$ expresses that cell k is strongly constrained by national policy, otherwise, $CP_{u,k,t} = 1$.

2.3. Model implementation

In this study, TSDM is designed and implemented in the Logo language based on the NetLogo platform. NetLogo is modeling software based on the Logo programming language for model development, and is used as a platform to simulate and model various natural and social phenomena over time (Wilensky, 1999). NetLogo was developed in 1999 and has been continuously updated

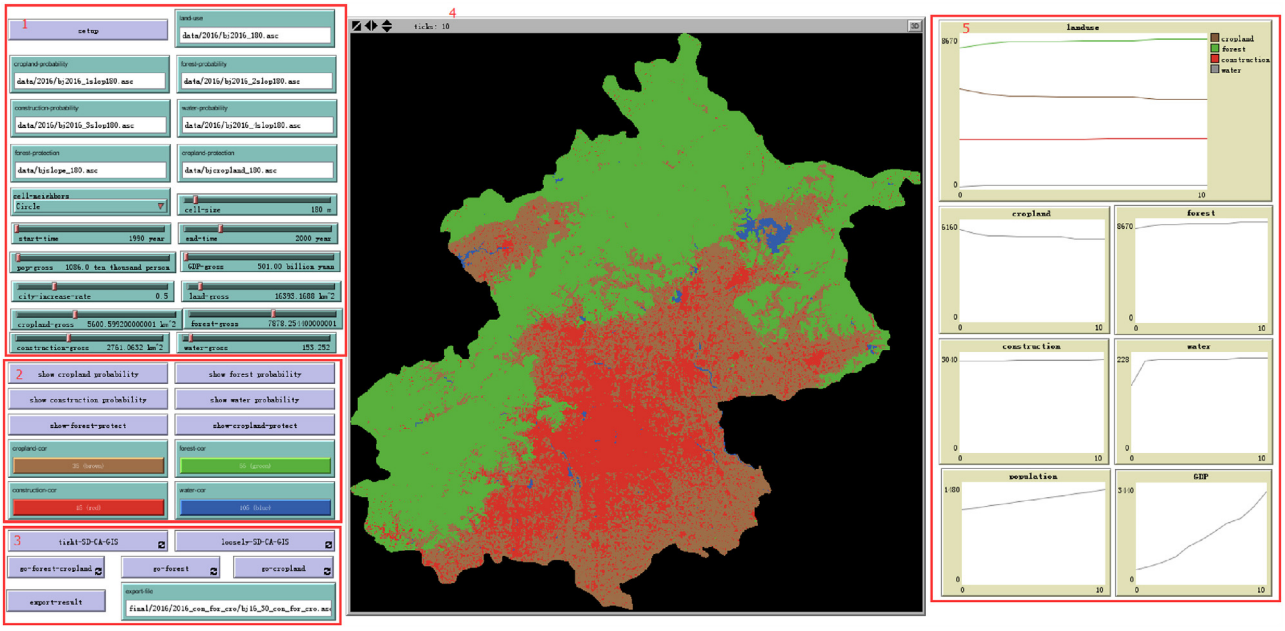

Fig. 3. Graphic TSDM user interface.

Table 1
Functions of the graphical TSDM user interface.

Modules	Function Description
Module 1	Sets different simulation scenarios by specifying original images and initial values of various variables.
Module 2	Displays probabilities of different land uses impacted by driving factors, national policies, and other macro-factors.
Module 3	Operates the evolution function of the model and outputs model results under different policy scenarios.
Module 4	Displays the dynamically land use and cover conditions based on the time step.
Module 5	Monitors the changes of land-use areas, population, and gross domestic product (GDP) for different simulation scenarios.

at Northwestern University. Compared with other platforms that simulate SD and CA, NetLogo has an extensive model library and is easy to learn and use. In addition, it can easily integrate SD, CA, and other models and extend GIS data. NetLogo can build complex models and graphical interfaces and incorporates a simple but powerful programming language. NetLogo has been extensively used to propose complex models for land use and urban expansion (Feitosa et al., 2011; Le et al., 2008).

The TSDM, as based on the NetLogo platform (Fig. 3), has a friendly visual user interface. The model is composed of five main modules; the module functions are listed in Table 1. Users can freely set up parameters of this model to create and group a variety of simulation scenarios. The results are obtained in the form of dynamic images and data in the view box and monitors. Users can scrutinize dynamics and intuitively comprehensible results showing the impact of policy, population, and other macro-factors. Also, the model can also output standard map data and globally variable statistical results at specified time points; this allows further map analysis and statistical operations using other software (such as ArcGIS and SPSS).

3. Results

3.1. Study area and data

Beijing is located in the North China Plain and is the nation's political, economic, and cultural center. The city is also the center of the Jingjinji metropolitan region. The population of Beijing has been increasing in recent years. According to official statistics, the permanent population in Beijing has increased to 21.7 million by the end of 2015, which includes a permanent migrant population of 8.23 million. On one hand, the population increase promotes the growth of the gross domestic product (GDP) in Beijing. In 2015, the GDP increased to 2296.86 billion yuan; nearly 7% more than in the previous year. On the other hand, an excessive population causes economic, transportation, housing, and water shortage and other issues. To alleviate these problems, the government has published a series of policies and regulations including a household registration deflation policy and an economic adjustment policy. However, whether these policies can really alleviate these problems or enhance the sustainable development of the city is yet to be determined.

Data collection over a large time interval is important in land-use simulation (Verburg et al., 1999). Hence, four remote sensing images provided by Landsat-5, Landsat-7, and Landsat-8 were used in this study, which include remote data for 1990, 2000, 2010, and 2016. The spatial resolution of the images acquired from the U.S. Geological Survey is 30 m. This study also used global 30 m Digital Elevation Model (DEM) data, which were obtained from the Geospatial Data Cloud. In addition, a vector data series was selected including the distribution of highways, airports, parks, hospitals, and government offices. Previous studies have shown that these vector factors are closely related to the urban land-use change (White and Engelen, 1993; Wu and Webster, 1998). Detailed information about the data used is listed in Table 2. For operational accuracy and reliability of the model, coordinate systems of all vector data were defined in the Universal Transverse Mercator (UTM) coordinate system.

To simplify the model, the remote sensing images from 1990 to 2016 were categorized into four main land types in this study: cropland, forest land, construction land, and water. To improve the classification precision and avoid the misclassification of land

Table 2
Detailed information about the data used in this study.

Data	Data Source	Resolution
Landsat images	U.S. Geological Survey	30 m
Digital Elevation Model	Geospatial Data Cloud	30 m
Highway network	Beijing municipal government data resource network	30 m
Hospital features	Beijing municipal government data resource network	30 m
Park features	Beijing municipal government data resource network	30 m
Airport features	Beijing municipal government data resource network	30 m
Government offices	Beijing municipal government data resource network	30 m
Population	Beijing Statistical Yearbook	
Gross Domestic Product	Beijing Statistical Yearbook	

Table 3
Areal land-use changes for Beijing from 1990 to 2016.

	Cropland	Forest	Construction	Water
1990 (km^2)	5621.69	8576.25	1991.24	203.89
2000 (km^2)	5275.92	8803.37	2088.67	224.99
2010 (km^2)	4441.78	8539.28	3180.09	230.59
2016 (km^2)	3676.07	8932.10	3593.35	150.40
Change in Area (km^2)	−1945.62	355.85	1602.11	−53.49

types, Google Earth images were used for comparison. The overall classification accuracies are 92.31%, 97.60%, 94.47%, and 93.26% for 1990, 2000, 2010, and 2016, respectively. Also, the interpreted raster data were resampled at 180 m to take the data loading and computing time in NetLogo into account and ensure that enough spatial details would be obtained (He et al., 2006).

The areal land-use changes in Beijing from 1990 to 2016 are shown in Table 3. The cropland area decreased by 1945.62 km^2, while the construction land area increased by 1602.11 km^2. Small changes were observed for the forest land and water areas. This may indicate that the construction land occupied parts of the cropland in Beijing due to the excessive population and economic development.

3.2. Simulation results

It is necessary to validate the model with existing data before using it to simulate and predict land-use change to ensure the authenticity of the simulation (Li and Liu, 2006). In this study, land-use data from 1990 to 2016 were analyzed, with the data from 1990 and 2000 used as training data, whereas the data from 2010 were employed as test data. The training data were used to test and calibrate various parameters and transition rules of the model, whereas the test data were used to verify the calibrated model.

According to the significance index and other evaluation indexes, obtained from logistic regression results in SPSS, six environmental variables, including distance to highways, distance to hospitals, distance to parks, distance to airports, distance to government offices, and slope were chosen. The units of these factors were not consistent. The six factors were therefore normalized, eliminating effects caused by different units. Based on the logistic regression Equations (8) and (9), the probability of being affected by environmental factors was calculated for each land-use type from 1990 to 2016:

$$P_E = \frac{1}{1+\exp(-z)} \tag{8}$$

$$z = \alpha + \sum_{i=1}^{n} \beta_i X_i \tag{9}$$

where P_E represents the influence of the surrounding environment on the cell land type; α indicates the logistic regression constant; β_i denotes the logistic regression coefficient of some environmental features; and X_i is the influence of some environmental factors (e.g., the distance to hospitals).

At the same time, the effects of SD macro-driving factors on CA micro-transition rules were taken into account. The CA transition rules were modified according to the changes of cropland, forest, population, and other economic features in SD. The population changes, land changes, and other macro-scale factors were seamlessly integrated with micro-land allocation to quantitatively solve questions.

To simplify the TSDM, we assumed that the change of each land type in SD was influenced by a single human society factor. In the SD model, the land-use changes in Beijing were predicted mainly based on population policy, economic policy, land policy, and other macro-government regulations (Fig. 4). The Beijing Statistical Yearbook and Beijing land-use distribution were used to determine the causal relationships and system equations of the SD model.

After the CA model and the SD model were proposed, the two submodels were seamlessly integrated within GIS. The GIS data were first loaded into the model to set the initial parameters. The SD model was then employed to predict the land-use area of the next year and the area of each land-use type was transferred to the CA model to influence the CA transition rules. The CA iterations were controlled by the land area values during the operation of the CA model. When the CA had completed its iteration, the land area values calculated in CA were fed back to the SD model. The simulation was then advanced to the next year until the scheduled simulation year was reached.

Common methods to verify the accuracy of the simulation results are visual and point-by-point comparisons (Wu, 2002). Although visual inspection has some subjectivity, the overall quality of the simulation results can be easily assessed (Clarke et al., 1997; Ward et al., 2000). Based on the visual comparison, the simulation results (Fig. 5) reflect the spatial patterns of the actual data well, although several scattered land phenomena were not well simulated. A point-by-point comparison was adopted in this study to quantify the consistency between the simulation and actual results. The simulation was compared with the real data of the corresponding year; the consistency between the simulation data and original data was determined by calculating a *kappa* coefficient. The *kappa* coefficient is defined as follows (Congalton, 1991):

$$kappa = \frac{N\sum_{i=1}^{r} x_{ii} - \sum_{i=1}^{r}(x_{i+} * x_{+i})}{N^2 - \sum_{i=1}^{r}(x_{i+} * x_{+i})}, \tag{10}$$

where N is the total number of elements in the error matrix; r represents the rows of the error matrix; x_{ii} are the elements in the main diagonal of the error matrix, which are the elements with simulation results equal to the true results; x_{i+} is the sum of the elements in row i of the error matrix; and x_{+i} is the sum of the elements in column i of the error matrix.

The simulation precision of land-use data for 2000, 2010, and 2016 reached 83.75%, 80.98%, and 77.40% and the *kappa* coefficients were 0.7144, 0.6775, and 0.6300, respectively. Furthermore, Table 4 shows the quantitative results for the simulated area for 2000, 2010, and 2016 and the simulated error. The simulation accuracies are higher than in previous studies (Chen et al., 2002; Han

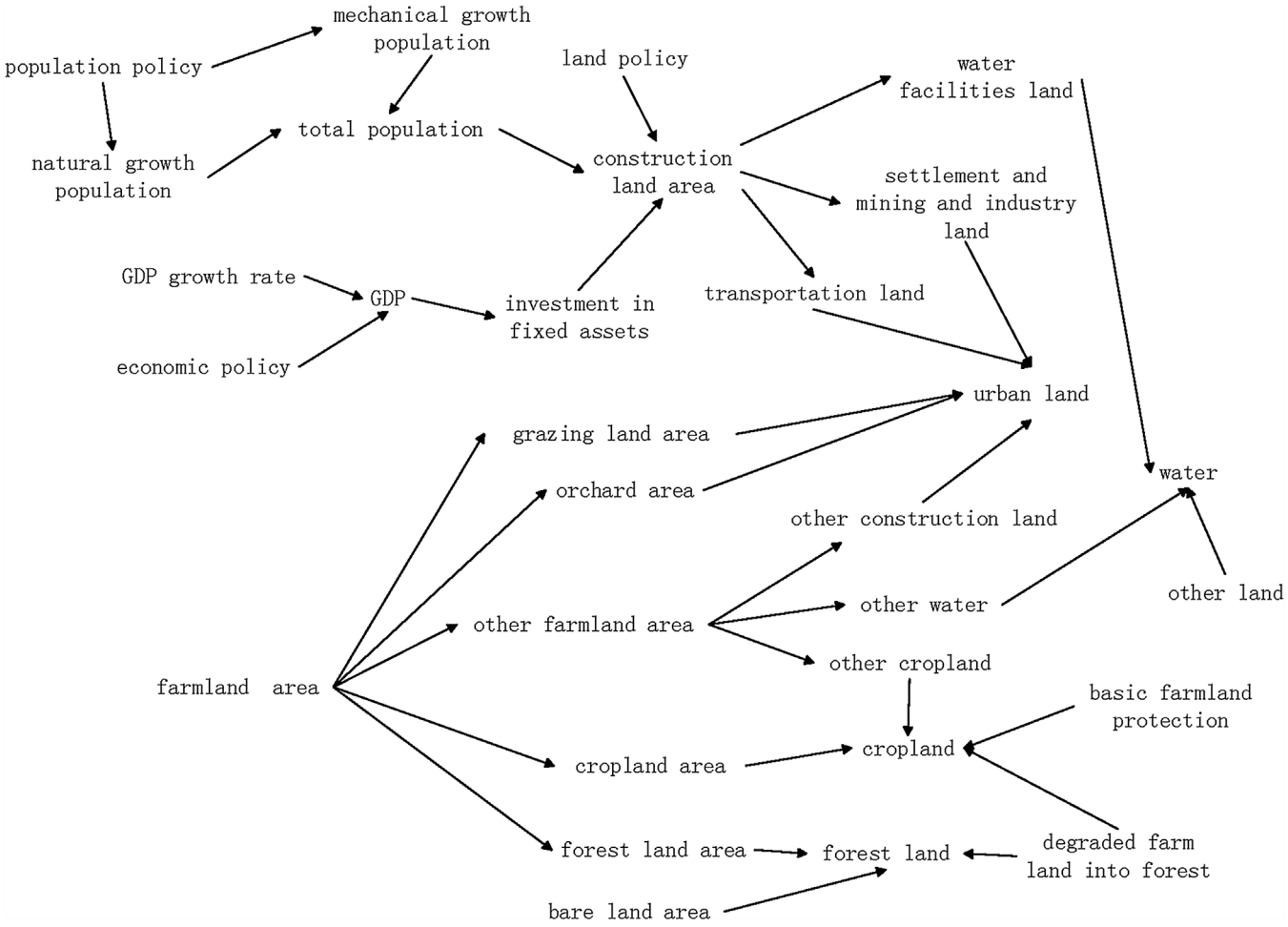

Fig. 4. SD causality diagram for land use in Beijing.

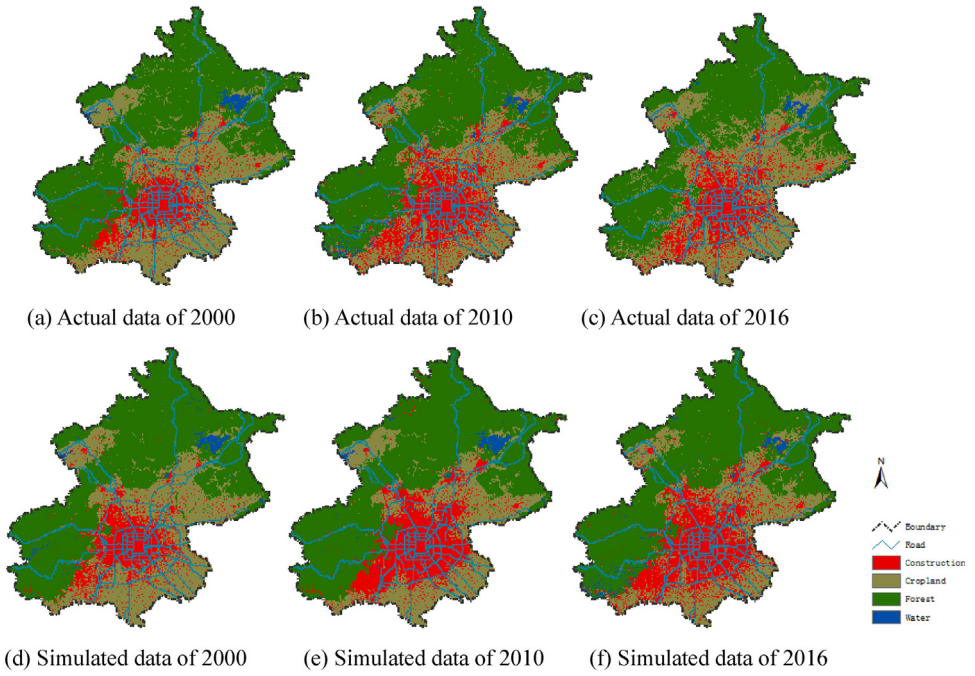

Fig. 5. Land-use change simulation for Beijing from 2000 to 2016.

Table 4
Simulated results for 2000 and 2016 in Beijing.

		Cropland	Forest	Construction	Water
2000	Simulated Area (km^2)	5133.52	8753.61	2302.05	203.89
	Error	0.0270	0.0057	0.1022	0.0938
2010	Simulated Area (km^2)	3785.16	8973.34	3409.45	224.99
	Error	0.1478	0.0508	0.0721	0.0243
2016	Simulated Area (km^2)	3680.80	8695.67	3784.68	230.59
	Error	0.0013	0.0265	0.0532	0.5332

et al., 2009; Liu et al., 2008). The simulation accuracies for 1990 and 2000 were higher than the accuracy of 2010 because the model correction is based on the training data from 1990 and 2000. However, the classification accuracy and other parameters of remote sensing images affect the model simulation accuracy differently.

The simulation results (Fig. 5 and Table 4) show that the main land-use change from 1990 to 2016 is the expansion of urban construction land. Some of the forest and cropland in Fangshan and Daxing was disturbed by the center of urban expansion. The economy has developed rapidly and the urban population has increased substantially since the reform and opening-up policy in 1978. As the national political, economic, and cultural center, Beijing has a large influx of migrant workers, causing urban over expansion. Meanwhile, people ignore and underrate the great significance of cropland and the green belt for urban sustainable development and a lot of farmland and green space have been occupied. The urban development in Beijing does not form a decentralized multi-center pattern. On the contrary, the cohesion effect of the central district is enhanced and multiple subdistricts merged to form a "big-pie" development pattern.

The development of Beijing has attracted the attention of many scholars (Chen et al., 2002; He et al., 2005). The attraction and cohesion of the central urban district and the construction of ring roads in Beijing slowed the development of satellite towns down. Over-expansion of the central urban district and environmental degradation occurred; the achievement of a sustainable development of Beijing is problematic.

4. Discussion

In this study, TSDM was proposed and developed to achieve bidirectional communication between SD and CA. The comparison of the TSDM with the traditional SD–CA integrated model confirms that TSDM has a better simulation accuracy. The TSDM is implemented based on the NetLogo platform in which users can simulate different land-use policies by setting different parameters to obtain land-use changes under different conditions.

4.1. Data bidirectional communication between SD and CA

Bidirectional communication can be implemented in TSDM by selecting appropriate indicators as communication mechanisms between SD and CA. When the model begins to run, the SD transmits the calculation results of the indicators to the CA to control the evolution of the CA. After a time step, the operational results of the indicators in CA are fed back to SD to modify the causalities and dynamic equations in SD. This cycle is repeated to achieve the bidirectional communication between the SD and CA models and solve the problems of the one-way communication model of the traditional SD–CA integrated model that only relies on indicators from SD to control the CA iterations.

In this study, we took the urban construction area as an example to illustrate the effect of the interactive communication between SD and CA. Fig. 6 shows that the construction area obtained from the system equations in SD is transferred to CA based on the land-use data for 1990. After the value reaches the CA model, it becomes part of the influencing factors used to determine the CA transition rules, addressing the drawback that CA transition rules never change during the whole simulation. Meanwhile, the CA iterations are controlled by the area and other variables. When the CA iterations are terminated, the construction area in the land-use distribution map is calculated by integrating CA with GIS and fed back to SD to modify the causalities and system equations of SD. For comparison, the evolution of the land distribution in CA was simulated without influences from SD. To facilitate the comparison, a small part of the land-use area in Beijing has been selected for display in Fig. 6. The comparison of the two land-use maps shows that the SD indexes change the distribution and variations of the land use.

Table 5
Comparison between TSDM and traditional SD–CA model.

	TSDM		Traditional SD–CA model	
	Precision	*kappa* coefficient	Precision	*kappa* coefficient
2000	83.75%	0.7144	82.08%	0.6881
2010	80.98%	0.6775	77.70%	0.6265
2016	77.40%	0.6300	76.17%	0.6109

4.2. Comparison with traditional SD-CA integrated model

The integration of the SD and CA models can be widely used to simulate complex and nonlinear geographical phenomena (Han et al., 2009; He et al., 2006). As a contrast test, the traditional SD–CA integrated model in this study used the same data, transition rules in CA, and system equations in SD as those applied in TSDM.

It is hard to quantitatively differentiate the simulation precision of TSDM and the traditional SD–CA integrated model by visual comparison; thus, a point-by-point method was used. Table 5 shows the simulation precision and *kappa* coefficient for the TSDM and traditional SD–CA model. The overall simulation precision of the traditional SD–CA model is lower than that of TSDM; the same is true for the *kappa* coefficient.

The comparison indicates that TSDM has a much better ability to model the land-use change. The TSDM is a more practical approach for the integration on the cell-level, simulating both the overall amount and the spatial distribution of the land-use change.

4.3. Setting simulation scenarios by changing parameters

The TSDM can be used to set up different simulation scenarios by adjusting the parameters. By this approach various alternative, land-use patterns in Beijing can be easily and quickly obtained and displayed. The main land-use changes in Beijing from 1990 to 2000 were simulated by taking the population indicators as an example and setting the ideal Beijing population to 23 million, 30 million, and 40 million, respectively (Fig. 7). In the monitors and view box, the land distribution and related data can be intuitively accessed. The change of construction area, cropland, and forest area in Beijing can also be displayed. The land-use conditions of construction area, cropland, and forest area in Beijing from

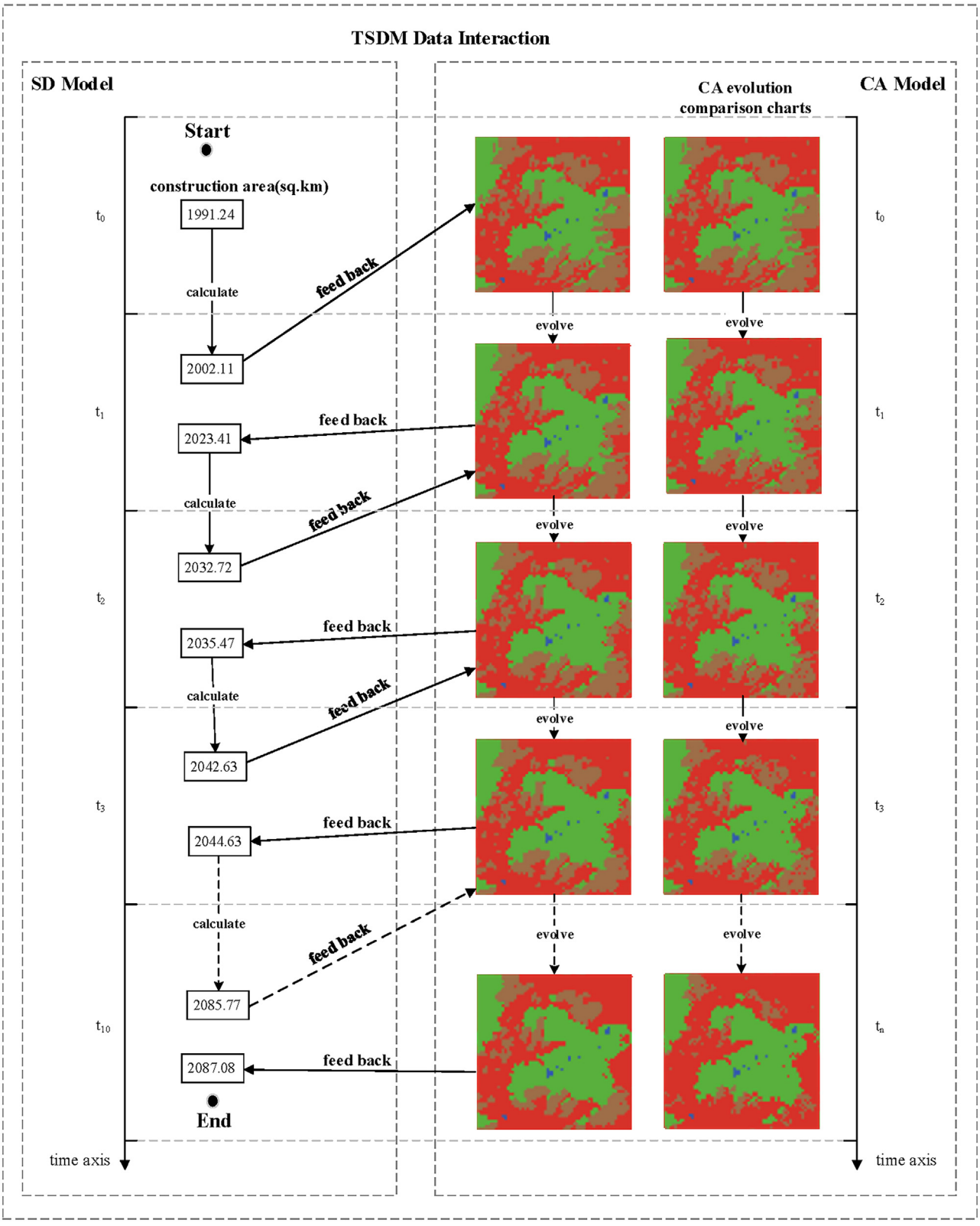

Fig. 6. Bidirectional communication process between SD and CA in the TSDM. The CA evolution comparison charts show the evolution results in CA without influences from SD.

1990 to 2000 were acquired by using the construction area as an indicator and setting the Beijing maximum construction area to 3000 km^2, 4000 km^2, and 5000 km^2, respectively (Fig. 8). The simulation results in Figs. 7 and 8 show that the construction area increased and the cropland and forest area decreased with the increase of the ideal population or maximum construction area in Beijing.

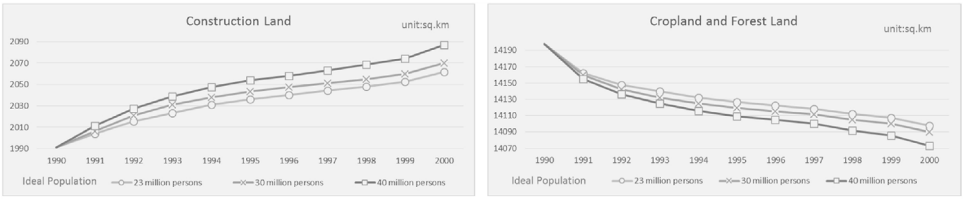

(a) Construction Area (b) Cropland and Forest Area

Fig. 7. Land-use conditions for different population constraints.

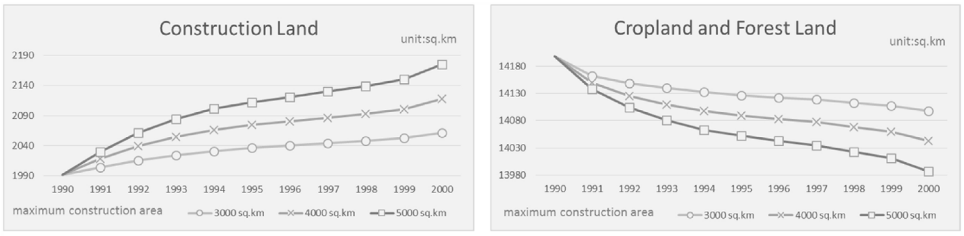

(a) Construction Area (b) Cropland and Forest Area

Fig. 8. Land-use conditions for different construction area constraints.

Various land-use distributions can be obtained in TSDM by setting different populations, construction areas, and other parameters. We can search for the most suitable combination of parameters for the urban development in Beijing using the different simulation results. The operation and use of the TSDM implemented on the NetLogo platform is convenient for users; the TSDM is also flexible with respect to setting parameters and can provide a basis and reference for the government to formulate relevant policies.

5. Conclusions

The "top-down" SD model and "bottom-up" CA model have been widely used in various complex land-use simulations. In this study, the TSDM facilitates the data interaction between SD and CA at the cell-level; thus, the two models have bidirectional communication and mechanistic coupling. The TSDM realizes the seamless coupling among SD, CA, and GIS by using GIS to visually express the spatial data. Meanwhile, the land-use changes can be obtained for "what-if" scenarios by setting different simulation parameters and original conditions based on the characteristics of the SD. The simulation results in this study were compared with previous similar experiments and the traditional SD–CA integrated model. The results of the comparison show that the TSDM simulates the spatio-temporal land-use change better and has a higher precision and *kappa* coefficient; it reflects the development of the objective world better.

The synergy of the steps between SD and CA is especially important for the operation of the whole model. The determination of the SD and the CA steps directly influences the precision of the model simulation and the accuracy of the prediction results. At the same time, the scale of the cells also affects the simulated results. The local-scale data can improve the simulating precision and express more details of the objective world. However, the amount of raster data increases with increasing resolution; this adversely affects the operational speed of the model. The use of broad-scale data is associated with the omission of some details and the combination of fragmented information and greatly reduces the computing time. However, the use of broad-scale data will inevitably affect the accuracy of the simulation results and the expression of detailed spatial data. It is thus important to find a balance between the simulation accuracy and computing speed. NetLogo does not have a good solution for this problem. In future work, a TSDM-specific tool will be developed on the .NET platform based on C# language and will, if possible, be combined with parallel computing, which might not only improve the model precision but also exclude an effect on the computing speed.

In this paper, the TSDM was tested for the case of Beijing. The results show that the urban fringe is partly occupied by the overexpansion of urban construction land because of the strong condensation effect of the central urban district, construction of the Beijing ring road, and underestimation of the value of cultivated and green land. Beijing does not show the mutual development pattern of a central urban district and multi-satellite town. On the contrary, the central urban district merged with the subcentral urban district to form a bigger central urban area. In future urban development, the government should take a variety of coercive measures to effectively solve the problems of food security, water shortage, and environmental deterioration to achieve a healthy and sustainable development of Beijing.

Acknowledgements

This research was supported by the Chinese National Major Programs of International Cooperation and Exchanges of China (Grant No. S2015ZR1018), the National Natural Science Foundation of China (Grant No. 41601432), Beijing Natural Science Foundation (Grant No. 8174074), and the Key Laboratory of Spatial Data Mining & Information Sharing of Ministry of Education, Fuzhou University (Grant No. 2017LSDMIS06).

References

An, L., Linderman, M., Qi, J., Shortridge, A., Liu, J., 2005. Exploring complexity in a human–environment system: an agent-based spatial model for multidisciplinary and multiscale integration. Ann. Assoc. Am. Geogr. 95, 54–79.

Arsanjani, J.J., Helbich, M., Kainz, W., Boloorani, A.D., 2013. Integration of logistic regression, Markov chain and cellular automata models to simulate urban expansion. Int. J. Appl. Earth Obs. Geoinf. 21, 265–275.

Chen, J., Gong, P., He, C., Luo, W., Tamura, M., Shi, P., 2002. Assessment of the urban development plan of Beijing by using a CA-based urban growth model. Photogramm. Eng. Remote Sens. 68, 1063–1072.

Clarke, K.C., Gaydos, L.J., 1998. Loose-coupling a cellular automaton model and GIS: long-term urban growth prediction for San Francisco and Washington/Baltimore. Int. J. Geogr. Inf. Sci. 12, 699–714.
Clarke, K.C., Hoppen, S., Gaydos, L., 1997. A self-modifying cellular automaton model of historical urbanization in the San Francisco Bay area. Environ. Plan. B: Plan. Des. 24, 247–261.
Congalton, R.G., 1991. A review of assessing the accuracy of classifications of remotely sensed data. Remote Sens. Environ. 37, 35–46.
Feitosa, F.F., Le, Q.B., Vlek, P.L.G., 2011. Multi-agent simulator for urban segregation (MASUS): A tool to explore alternatives for promoting inclusive cities. Comput. Environ. Urban Syst., 104–115.
Guo, H., Liu, L., Huang, G., Fuller, G., Zou, R., Yin, Y., 2001. A system dynamics approach for regional environmental planning and management: a study for the Lake Erhai Basin. J. Environ. Manag. 61, 93–111.
Han, J., Hayashi, Y., Cao, X., Imura, H., 2009. Application of an integrated system dynamics and cellular automata model for urban growth assessment: a case study of Shanghai, China. Landsc. Urban Plann. 91, 133–141.
He, C., Shi, P., Chen, J., Li, X., Pan, Y., Li, J., Li, Y., Li, J., 2005. Developing land use scenario dynamics model by the integration of system dynamics model and cellular automata model. Sci. China Ser. D: Earth Sci. 48, 1979–1989.
He, C., Okada, N., Zhang, Q., Shi, P., Zhang, J., 2006. Modeling urban expansion scenarios by coupling cellular automata model and system dynamic model in Beijing, China. Appl. Geogr. 26, 323–345.
Hu, Y., Zheng, Y., Zheng, X., 2013. Simulation of land-use scenarios for Beijing using CLUE-S and Markov composite models. Chin. Geogr. Sci. 23, 92–100.
Hui-Hui, F., Hui-Ping, L., Ying, L., 2012. Scenario prediction and analysis of urban growth using SLEUTH model. Pedosphere 22, 206–216.
López, E., Bocco, G., Mendoza, M., Duhau, E., 2001. Predicting land-cover and land-use change in the urban fringe: a case in Morelia city Mexico. Landsc. Urban Plan. 55, 271–285.
Lauf, S., Haase, D., Hostert, P., Lakes, T., Kleinschmit, B., 2012. Uncovering land-use dynamics driven by human decision-making–A combined model approach using cellular automata and system dynamics. Environ. Model. Softw. 27, 71–82.
Le, Q.B., Park, S.J., Vlek, P.L.G., Cremers, A.B., 2008. Land-Use Dynamic Simulator (LUDAS): A multi-agent system model for simulating spatio-temporal dynamics of coupled human–landscape system. I. Structure and theoretical specification. Ecol. Inf., 135–153.
Le, Q.B., Park, S.J., Vlek, P.L.G., 2010. Land Use Dynamic Simulator (LUDAS): A multi-agent system model for simulating spatio-temporal dynamics of coupled human–landscape system: 2. Scenario-based application for impact assessment of land-use policies. Ecol. Inf., 203–221.
Li, X., Gar-On Yeh, A., 2004. Data mining of cellular automata's transition rules. Int. J. Geogr. Inf. Sci. 18, 723–744.
Li, X., Liu, X., 2006. An extended cellular automaton using case-based reasoning for simulating urban development in a large complex region. Int. J. Geogr. Inf. Sci. 20, 1109–1136.
Li, X., Chen, Y., Liu, X., Li, D., He, J., 2011. Concepts, methodologies, and tools of an integrated geographical simulation and optimization system. Int. J. Geogr. Inf. Sci. 25, 633–655.
Li, X., Liu, X., Yu, L., 2014. A systematic sensitivity analysis of constrained cellular automata model for urban growth simulation based on different transition rules. Int. J. Geogr. Inf. Sci. 28, 1317–1335.
Liao, J., Tang, L., Shao, G., Su, X., Chen, D., Xu, T., 2016. Incorporation of extended neighborhood mechanisms and its impact on urban land-use cellular automata simulations. Environ. Model. Softw, 163–175.
Liu, X., Li, X., Liu, L., He, J., Ai, B., 2008. A bottom-up approach to discover transition rules of cellular automata using ant intelligence. Int. J. Geogr. Inf. Sci. 22, 1247–1269.
Liu, X., Li, X., Shi, X., Zhang, X., Chen, Y., 2010. Simulating land-use dynamics under planning policies by integrating artificial immune systems with cellular automata. Int. J. Geogr. Inf. Sci., 783–802.
Liu, X., Ou, J., Li, X., Ai, B., 2013. Combining system dynamics and hybrid particle swarm optimization for land use allocation. Ecol. Model. 257, 11–24.
Munshi, T., Zuidgeest, M., Brussel, M., van Maarseveen, M., 2014. Logistic regression and cellular automata-based modelling of retail commercial and residential development in the city of Ahmedabad, India. Cities 39, 68–86.
Shen, T., 2006. China urban future simulation: an integrated framework of CGE and GIS. Adv. Earth Sci. 21.
Theobald, D.M., Gross, M.D., 1994. EML: a modeling environment for exploring landscape dynamics. Computers. Environ. Urban Syst. 18, 193–204.
Verburg, P., Veldkamp, A., Fresco, L., 1999. Simulation of changes in the spatial pattern of land use in China. Appl. Geogr. 19, 211–233.
Ward, D.P., Murray, A.T., Phinn, S.R., 2000. A stochastically constrained cellular model of urban growth. Computers. Environ. Urban Syst. 24, 539–558.
Weng, Q., 2002. Land use change analysis in the Zhujiang Delta of China using satellite remote sensing, GIS and stochastic modelling. J. Environ. Manag. 64, 273–284.
White, R., Engelen, G., 1993. Cellular automata and fractal urban form: a cellular modelling approach to the evolution of urban land-use patterns. Environ. Plan. A 25, 1175–1199.
White, R., Engelen, G., 2000. High-resolution integrated modelling of the spatial dynamics of urban and regional systems. Comput. Environ. Urban Syst. 24, 383–400.
White, R., Engelen, G., Uljee, I., 1997. The use of constrained cellular automata for high-resolution modelling of urban land-use dynamics. Environ. Plan. B: Plan. Des. 24, 323–343.
Wilensky, 1999. NetLogo. Center for Connected Learning and Computer-Based Modeling (CCL).
Wu, F., Webster, C.J., 1998. Simulation of land development through the integration of cellular automata and multicriteria evaluation. Environ. Plan. B: Plan. Des. 25, 103–126.
Wu, F., 2002. Calibration of stochastic cellular automata: the application to rural-urban land conversions. Int. J. Geogr. Inf. Sci. 16, 795–818.
Yang, X., Zheng, X.-Q., Lv, L.-N., 2012. A spatiotemporal model of land use change based on ant colony optimization, Markov chain and cellular automata. Ecol. Model. 233, 11–19.
Zhang, W., Huang, B., 2014. Land use optimization for a rapidly urbanizing city with regard to local climate change: shenzhen as a case study. J. Urban Plann. Dev. 141, 05014007.
Zhang, C., Chen, M., Li, R., Fang, C., Lin, H., 2016. What's going on about geo-process modeling in virtual geographic environments (VGEs). Ecol. Model. 319, 147–154.
Zheng, X., 2012. On the geographic system simulation basic model. Chin. J. Nat. 34, 143–149.